Published in final edited form as:

Mol Cancer Ther. 2015 July ; 14(7): 1650–1660. doi:10.1158/1535-7163.MCT-15-0067.

AGS67E, an Anti-CD37 Monomethyl Auristatin E Antibody–Drug Conjugate as a Potential Therapeutic for B/T-Cell Malignancies and AML: A New Role for CD37 in AML

Daniel S. Pereira[1], **Claudia I. Guevara**[1], **Liqing Jin**[2], **Nathan Mbong**[2], **Alla Verlinsky**[1], **Ssucheng J. Hsu**[1], **Hector Aviña**[1], **Sher Karki**[1], **Joseph D. Abad**[1], **Peng Yang**[1], **Sung-Ju Moon**[1], **Faisal Malik**[1], **Michael Y. Choi**[3], **Zili An**[1], **Kendall Morrison**[1], **Pia M. Challita-Eid**[1], **Fernando Doñate**[1], **Ingrid B.J. Joseph**[1], **Thomas J. Kipps**[3], **John E. Dick**[2], and **David R. Stover**[1]

[1]Agensys Inc., an Affiliate of Astellas Pharma Inc., Santa Monica, California

[2]Princess Margaret Cancer Centre, University Health Network, and Department of Molecular Genetics, University of Toronto, Toronto, Ontario, Canada

[3]Division of Hematology-Oncology, University of California, San Diego, Moores Cancer Center, La Jolla, California

Abstract

CD37 is a tetraspanin expressed on malignant B cells. Recently, CD37 has gained interest as a therapeutic target. We developed AGS67E, an antibody–drug conjugate that targets CD37 for the potential treatment of B/T-cell malignancies. It is a fully human monoclonal IgG2 antibody

Corresponding Author: Daniel S. Pereira, Agensys Inc., an affiliate of Astellas Pharma Inc., 1800 Stewart Street, Santa Monica, CA 90404. Phone: 424-280-5296; Fax: 424-280-5040; dpereira@agensys.com.
Current Address for Ssucheng J. Hsu: Pharmacyclics Inc., Research Department, Sunnyvale, CA.

Note: Supplementary data for this article are available at Molecular Cancer Therapeutics Online (http://mct.aacrjournals.org/).

Disclosure of Potential Conflicts of Interest

J.E. Dick reports receiving commercial research grant from Agensys. No potential conflicts of interest were disclosed by the other authors.

Authors' Contributions

Conception and design: D.S. Pereira, S.J. Hsu, J.D. Abad, Z. An, K. Morrison, P.M. Challita-Eid, I.B.J. Joseph, T.J. Kipps, J.E. Dick, D.R. Stover

Development of methodology: C.I. Guevara, S. Karki, J.D. Abad, S.-J. Moon, Z. An, K. Morrison, P.M. Challita-Eid, I.B.J. Joseph, J.E. Dick

Acquisition of data (provided animals, acquired and managed patients, provided facilities, etc.): C.I. Guevara, L. Jin, N. Mbong, A. Verlinsky, H. Aviña, P. Yang, S.-J. Moon, M.Y. Choi, K. Morrison, I.B.J. Joseph, T.J. Kipps, J.E. Dick

Analysis and interpretation of data (e.g., statistical analysis, biostatistics, computational analysis): C.I. Guevara, L. Jin, S.J. Hsu, S. Karki, P. Yang, S.-J. Moon, M.Y. Choi, Z. An, K. Morrison, P.M. Challita-Eid, F. Doñate, I.B.J. Joseph, J.E. Dick

Writing, review, and/or revision of the manuscript: D.S. Pereira, C.I. Guevara, H. Aviña, P. Yang, M.Y. Choi, Z. An, K. Morrison, P.M. Challita-Eid, F. Doñate, I.B.J. Joseph, T.J. Kipps, J.E. Dick, D.R. Stover

Administrative, technical, or material support (i.e., reporting or organizing data, constructing databases): D.S. Pereira, C.I. Guevara, A. Verlinsky, S. Karki Study supervision: D.S. Pereira, C.I. Guevara, A. Verlinsky, S.J. Hsu, Z. An, K. Morrison, F. Donāte, I.B.J. Joseph, D.R. Stover

Other (sequenced original hybridoma, confirmed sequence a second time, and humanized the v-mice Ab sequences by replacing the mouse Fc regions with human sequences; subsequently cloned the heavy and light chains into CHO cell line production plasmids, and then confirmed those constructs): F. Malik

(AGS67C) conjugated, via a protease-cleavable linker, to the microtubule-disrupting agent monomethyl auristatin E (MMAE). AGS67E induces potent cytotoxicity, apoptosis, and cell-cycle alterations in many non-Hodgkin lymphoma (NHL) and chronic lymphocytic leukemia (CLL) cell lines and patient-derived samples *in vitro*. It also shows potent antitumor activity in NHL and CLL xenografts, including Rituxan-refractory models. During profiling studies to confirm the reported expression of CD37 in normal tissues and B-cell malignancies, we made the novel discovery that the CD37 protein was expressed in T-cell lymphomas and in AML. AGS67E bound to >80% of NHL and T-cell lymphomas, 100% of CLL and 100% of AML patient-derived samples, including $CD34^{+}CD38^{-}$ leukemic stem cells. It also induced cytotoxicity, apoptosis, and cell-cycle alterations in AML cell lines and antitumor efficacy in orthotopic AML xenografts. Taken together, this study shows not only that AGS67E may serve as a potential therapeutic for B/T-cell malignancies, but it also demonstrates, for the first time, that CD37 is well expressed and a potential drug target in AML.

Introduction

The CD37 antigen is a transmembrane protein of the tetraspanin superfamily that is highly expressed on B cells during the pre-B to peripheral mature B-cell stages, but is absent on early B progenitor cells or terminally differentiated plasma cells (1, 2). It is weakly expressed in a subset of peripheral blood mononuclear cells (PBMC) and in tissues where lymphocytes reside/infiltrate (1). Although the exact physiologic role of CD37 is unclear, it has been implicated as a signaling death receptor (3), and observations from knockout mice suggest that it is not essential for B-cell development, but may function to regulate B/T-cell interactions/proliferation as well as aspects of humoral and cellular immune responses (4, 5). With respect to cancer, CD37 is highly expressed on malignant B cells in non-Hodgkin lymphoma (NHL) and chronic lymphocytic leukemia (CLL; ref. 6). Consequently, CD37 represents a promising therapeutic target for B-cell malignancies.

Anti-CD20 antibodies, such as rituximab, of a tumumab, and obinutuzamab, have proven to be effective for the treatment of NHL and CLL, either as single agents or in combination therapy (7, 8). The intrinsic anticancer activities of these antibodies include direct signaling/proapoptotic activity, antibody-dependent cell-mediated cytotoxicity (ADCC), and complement-dependent cytotoxicity. However, many patients eventually relapse or experience resistance to available treatments, creating a need for additional therapeutic options. The clinical experience with CD37 targeted agents is still in its infancy and is as follows: (i) radioimmunotherapy with ^{131}I-MB-1 in patients with NHL who experienced relapse resulted in some limited clinical responses, but this agent was not further developed as a therapeutic drug (9, 10); (ii) a CD37-binding small modular immunopharmaceutical protein (TRU-016) with apoptosis and ADCC-inducing abilities has advanced into clinical testing as a treatment for B-cell malignancies (11); (iii) an Fc-engineered antibody to CD37 (BI836826), also with ADCC and apoptosis-inducing functionality, is in early development (12); (iv) IMGN-529, an antibody–drug conjugate that combines the intrinsic proapoptotic and immune effector activities of its anti-CD37 antibody component with the cytotoxic potency of its DM1 maytansinoid payload, is also in development (13).

Encouraged by the clinical successes of ADCETRIS (brentuximab vedotin; ref. 14) and KADCYLA (ado-trastuzumab emtansine; ref. 15), the currently approved ADCs targeting cancer, we have developed AGS67E, a fully human anti-CD37 IgG2 antibody conjugated to the potent microtubule-disrupting agent monomethyl auristatin E (MMAE) via reduced cysteines and the protease-cleavable linker maleimidocaproyl-valine-citrulline-p-aminobenzyloxycarbonyl. Unlike all other reported therapeutic CD37 antibodies, including the recently reported IMGN-529 ADC (13), the unconjugated antibody component of our ADC does not exhibit intrinsic apoptotic or ADCC activity. The activity of AGS67E derives from its MMAE payload, which is selectively delivered by a highly specific antibody (AGS67C). Once delivered, AGS67E induces apoptosis, cell-cycle alterations, and cytotoxicity *in vitro* as well as antitumor efficacy *in vivo*. Because the preclinical potency of our agent is similar or superior to the reported preclinical efficacy of other CD37 antibodies in similar models of B-cell malignancies (11–13), we postulated that adding ADCC and apoptosis-inducing capabilities to our unconjugated antibody was unnecessary, and further that it could prove to be a liability from a toxicology or pharmacokinetic perspective.

Aside from a novel CD37 ADC that we report here, we also report, for the first time, that CD37 is well expressed in T-cell lymphomas and AML and that AGS67E exhibits potent antitumor efficacy in preclinical models of AML, including patient-derived models. Moreover, we show that CD37 is differentially expressed in $CD34^{+}CD38^{-}$ AML versus normal stem cells.

Taken together, our findings suggest that AGS67E may serve as a potential therapeutic for B/T-cell malignancies as well as AML. To our knowledge, this body of work is the first demonstrating that CD37 is well expressed and a potential drug target in AML.

Materials and Methods

IHC

IHC was used to evaluate CD37 expression in human lymphoma microarray samples (US Biomax) of formalin-fixed and paraffin-embedded (FFPE) tissue sections. Briefly, FFPE sections were deparaffinized, rehydrated, treated for antigen retrieval, and incubated with VCD37–9a73.1 (1 μg/mL), an in-house developed mouse anti-CD37 antibody or control IgG (1 μg/mL). Immunoreactivity was detected using a Super-Sensitive Polymer-HRP IHC Detection Kit (Biogenex Laboratories). Positivity was calculated by summing the percentage of tumor cells stained at a given staining intensity (0, negative; 1, weak; 2, moderate; 3, strong) multiplied by the weighted intensity to yield: high (201–300), moderate (101–200), low (1–100), and negative (0) H-scores.

Antibody generation, purification, and conjugation

Anti-CD37 antibodies were generated using standard hybridoma technology in genetically engineered VelocImmune mice humanized for the Ig locus (Regeneron Pharmaceuticals, Inc.) (16). The immunogen was 293T cells overexpressing human CD37. Following hybridoma screening, v67–6b15 was selected as the lead hybridoma from a fusion that yielded a total of 34 positives. It is cross-reactive to cynomolgus monkey but not rodent

CD37. To create a fully human antibody, total RNA was extracted from the antibody producing hybridoma cells using TRizol Reagent (Life Technologies) and the manufacturer's suggested protocol. cDNA synthesis was generated from total RNA using a RACE cDNA Amplification kit (Clontech) and a reverse primer within the constant region of the human light and heavy chains according to the manufacturer's protocol. The amplified variable human heavy and kappa light chains were sequenced and cloned into a mammalian cell expression vector encoding human IgG2 and kappa constant domains. The plasmid was transfected into CHOK1SV host cells (Lonza) to generate stable antibody (AGS67C) producing cell line. AGS67C was purified from conditioned CHO supernatant loaded onto a Protein A sepharose column. The antibody was eluted in 0.1 mol/L glycine, pH 3.5, and neutralized using 2 mol/l Tris, pH 9.0. To create AGS67E, AGS67C was conjugated with MMAE, linked to reduced cysteines of the antibody via a protease-cleavable linker, maleimidoca-proyl-valine-citrulline-p-aminobenzylcarbamoyl, as previously described (17). The drug:antibody ratio was 3:7. Once conjugated, AGS67E was purified from the reaction mixture using PD10 desalting columns.

Cell culture

DOHH-2 (ACC 47; lot 12, 2011), WSU-DLCL-2 (ACC 575; lot 4, 2009), SU-DHL-4 (ACC 495; lot 7, 2008), REC-1 (ACC 584; 2010), Granta-519 (ACC 342; lot 9, 2010), JVM-3 (ACC 18; lot 6, 2011), Molm-13 (ACC 554; lot 9, 2011), CMK (ACC 392; lot 8, 2012), Kasumi-1 (ACC 220; lot 13, 2011), PL-21 (ACC 536; lot 5, 2011), SKM-1 (ACC 547; lot 6, 2013), OCI-AML2 (ACC 99; lot 8, 2013), and UT-7 (ACC 137; lot 10, 2012) lines were obtained from the DSMZ. Mino (CRL-3000; 59427513, 2011), Raji (CCL-86; 58770576, 2011), Daudi (CCL-213; 58260721, 2011), Ramos (CRL-1596; 59352724, 2011), BDCM (CRL-2740; 58078622, 2012), MV4–11 (CRL-9591; 58352230, 2012), THP-1 (TIB-202; 59388245, 2012), Tf-1a (CRL-2451, 2012), KG-1 (CCL-246; 5803336, 2011), and Hel92.1.7 (TIB-180; 58736308, 2012) lines were obtained from the ATCC HL-60 (502350; 507608, 2010) and Molt-4 (507470, 2010) were from the NCI and EoL-1 (94042252, 2012) from Sigma/HPA. Cells were maintained at 37°C in a humidified 5% CO2 incubator and cultured in 10% FBS (Omega Scientific), RPMI-1640 (Gibco), 1 mmol/L Na Pyruvate, and 10 mmol/L HEPES (Gibco), with exception of THP-1 (10% FBS, RPMI-1640, 0.05 mmol/L β mercaptoethanol); Kasumi-1, PL-21, SKM-1 (20% FBS, RPMI-1640); MV4–11 [10% FBS, Iscove's modified Dulbecco's medium (IMDM)]; KG-1 (20% FBS, IMDM); OCI-AML2 (20% FBS, αMEM); and UT-7 (20% FBS αMEM, 5 ng/mL GM-CSF).

CLL samples were obtained from the CLL Research Consortium (CRC) at UCSD after patient consent. AML samples were obtained from the Ontario Cancer Institute after patient consent. Whole blood from normal healthy volunteers was obtained from the San Diego Blood Bank. PBMCs were prepared from these samples using standard procedures.

AGS67C binding measured using flow cytometry

Peripheral blood mononuclear cells—PBMCs (5×10^5) per test sample were incubated with Fc-Block, hIgG-Fc (100 μg/mL; Agensys), followed by incubation with AGS67C–Alexa 647-conjugated or isotype control antibody and commercially available fluorochrome-labeled antibodies (BD) according to manufacturer's recommendations.

Fluorochrome-labeled antibodies used were: CD20-FITC (B cells), CD56-AF488 (NK-cells), CD3-AF488 (T cells), CD14-FITC (monocytes), CD66-FITC (Neutrophils), and CD61-AF488 (platelets). Samples were acquired using the HTFC Screening System (Intellicyt). Mean fluorescence intensity ratio (MFIR) values (MFI of double-positive AGS67C-Alexa 647 over the MFI of double-positive isotype-Alexa 647) were plotted in GraphPad Prism.

Cell lines—Exponentially growing cell lines were harvested, reconstituted, and incubated for 1 hour on ice with biotinylated AGS67C and isotype control. Following a wash, R-PE-streptavidin was incubated for 1 hour, washed, and cells were analyzed on an Attune Acoustic Focusing Cytometer (Life Technologies). Data files were analyzed using FlowJo 7.6.5 software using standard gating. MFIR for CD37 expression was calculated by dividing the AGS67C–Biotin MFI by the isotype control–Biotin MFI.

Patient-derived CLL samples—Patient-derived CLL cells were incubated with AGS67C-Alexa 647–conjugated or isotype control antibody and costained with PE-conjugated anti-CD5 and FITC-conjugated anti-CD19 (BD Pharmigen) according to manufacturer's recommendations. Samples were acquired using Isotype-Alexa 647, CD5/CD19-positive gating for AGS67-Alexa 647–positive CLL samples. A FACS Calibur flow cytometer was used for acquisition, and data analysis was performed using FlowJo version 8.7. The CD19/CD5 double-positive B-cell population was gated to show AGS67C-positive cells, and MFIR for AGS67C was calculated by dividing the AGS67C-Alexa 647 MFI over the matched Isotype-Alexa 647 MFI. MFIR values for all samples were plotted in Graph Pad Prism 6, and sample MFIR distribution was analyzed by using column statistics.

Patient-derived AML samples—PBMCs from AML patients were isolated and incubated with a cocktail of CD45-FITC (BD), CD33-APC (BD), CD34-PE-Cy5 (Beckman Coulter), CD3-ECD (Beck-man Coulter), CD38-PE-Cy7 (BD), and either AGS67C-Biotin or isotype-Biotin antibodies. Secondary detection for biotinylated antibodies was accomplished with Streptavidin-PE. An LSRII flow cytometer (BD) was used for acquisition. Within the $CD45^+$ population, two distinct subpopulations were defined, $CD33^+/CD3^-/CD20^-$ (myeloid blasts) and $CD33^+/CD3^-/CD34^+/CD38^-$ [leukemic stem cells (LSC)]. Analysis was done with FlowJo version 9.5.4. MFIR for each AML sample was calculated by dividing the AGS67C MFI by the isotype MFI.

AGS67E *in vitro* cytotoxicity

Exponentially growing cells with a viability of 95% or greater were plated in fresh RPMI-1640 (Gibco-Invitrogen) media containing phenol red supplemented with 10% FBS (heat inactivated), 10 mmol/L Hepes, and 1 mmol/L sodium pyruvate. Cells were left overnight and treated with AGS67E and an isotype control. After 5 days of treatment and incubation at 37°C and 5% CO_2, cell viability was measured following a 1 hour incubation at 37°C with Presto Blue Reagent (Invitrogen). Samples were analyzed using a Synergy Microplate reader. Survival values were plotted using Graph-Pad Prism to calculate EC_{50} values that were derived using a curve-fitting analysis model for nonlinear curve regression, sigmoidal dose response with variable slope formula.

AGS67E cell-cycle analysis

Live cells were suspended in 250 μL RPMI-1640 (Gibco) media, 10% FBS, 10 mmol/L HEPES, and 1 mmol/L Na pyruvate, Hoechst 33342, trihydrochloride, trihydrate-10 mg/mL in water (Life Technologies). After 23 hours, cells were collected, resuspended in media containing diluted Hoechst 33342, and analyzed on an Attune cytometer harboring a 408 laser VL-1 detection. Data files were analyzed using FlowJo version 7.6.5 software, FSC-A vs. VL1-A.

AGS67E apoptosis

Exponentially growing cells were seeded in a 48-well plate overnight and resuspended in Annexin V Pac Blue and Sytox-7AAdvanced (Life Technologies), as recommended by the manufacturer. Following a 30-minute incubation, cells were acquired using an Attune cytometer with 405/VL-1 (Annexin V) and 488/BL-3 (Sytox-7AAdvanced) filter settings. Data files were analyzed using FlowJo version 7.6.5 software.

AGS67E cell line xenograft studies

Five- to 6-week-old female CB17/SCID mice (Charles River) were maintained and used at Agensys' animal facility using Institutional Animal Care and Use Committee (IACUC)-approved protocols. Depending on the cell line, 1–10e6 cells were injected into the flanks of individual SCID mice, and tumor volumes were allowed to reach 100 to 300 mm^3. Animals and their tumors were size matched and randomized into treatment and control groups. Depending on the study, AGS67E and an isotype control ADC were dosed by i.v. bolus injection either at 0.25, 0.75, 1.5, or 3.0 mg/kg at biweekly (BIW) or weekly (QW) frequencies and for a total of 2 to 4 doses. Tumor growth was monitored using caliper measurements every 3 to 4 days until the end of the study. Tumor volume was calculated as $width^2 \times length/2$, where width is the smallest dimension and length is the largest. Animals were euthanized when tumors reached 2,000 mm^3. Mean tumor volume data for each group were plotted over time with standard error bars. A statistical analysis of the tumor volume data for the last day before animal sacrifice was performed using the Kruskal–Wallis test. Pairwise comparisons were made using the Tukey test procedures (two-sided) to protect the experiment-wise error rate. This implementation of the Tukey test was performed on the ranks of the data. The percentage of tumor growth inhibition in each treated group versus a control group was calculated as follows: [(control – control baseline) – (treated – treated baseline)]/(control – control baseline) × 100%.

AGS67E AML patient–derived xenograft studies

NOD/SCID mice were bred and housed at the UHN/Princess Margaret Hospital (PMH; Toronto, Ontario, Canada) animal facility, and all studies were performed in accordance with guidelines approved by the UHN/PMH Animal Care Committee. Eight- to 12-week-old female NOD/SCID mice (10 per cohort) were sublethally irradiated (275 cGy) and interperitoneally injected with anti-CD122 antibody the day before intrafemoral transplantation. Freshly thawed primary AML samples harvested from patients' peripheral blood were transplanted at cell doses of 5e6/mouse. At day 21, post transplantation, AGS67E and an isotype control ADC were dosed by i.v. injection at 1.5 mg/kg, QW for a

total of 4 doses. Mice were sacrificed 7 days after the last treatment to assess the efficacy of AGS67E determined by the human AML engraftment in the injected right femur and non-injected bone marrow (left femur and two tibias). AML outgrowth was evaluated by flow cytometry using the following antibodies: CD45-FITC (BD), CD33-APC (BD), CD34-PE-Cy5 (Beckman Coulter), CD3-ECD (Beckman Coulter), CD38-PE-Cy7 (BD), and AGS67C-Biotin. Secondary detection of biotinylated antibodies utilized streptavidin–PE. Samples were analyzed using an LSRII flow cytometer (BD).

Results

CD37 expression in normal and cancer tissues

CD37 expression was evaluated in normal PBMCs (Fig. 1A) and normal solid tissues (Fig. 1B) using flow cytometry and IHC, respectively. Figure 1A shows strong staining for CD37 in $CD20^+$ B cells. In comparison, $CD56^+$, $CD3^+$, $CD14^+$, and $CD66^+$ cells showed 11-, 12-, 32-, and 28-fold less CD37 staining, respectively. CD37 staining was not observed on $CD61^+$ platelets.

To assess CD37 expression in normal solid tissues, 198 samples were tested, representing 32 human tissues. Figure 1B shows only those samples where CD37 expression was detected: lymph node, spleen, bone marrow, colon, small intestine, thymus, and tonsil (skin was incorporated as a negative control). These are tissues where lymphocytes are known to reside and it is these lymphocytes that were shown to express CD37.

With respect to CD37 expression in cancer tissues, Fig. 2A shows expression in human patient–derived lymphomas using IHC. Here, 85% (171 of 201) and 82% (14 of 17) of B-cell NHL and T-cell lymphoma samples exhibited CD37 positivity, respectively. Of the 171 positive B-cell NHL samples, 83 were diffuse large B-cell lymphomas (DBCL), 58 diffuse B-cell lymphomas, 7 mucosa-associated B-cell lymphomas, 5 nodular DBCL, 5 follicular lymphomas, 2 small lymphocytic lymphomas, 2 mantle cell lymphomas, 2 lymphocytic plasmacytoid lymphomas, 1 Burkitt lymphoma, and 6B–cell lymphomas (other). Of the 14 positive T-cell lymphoma samples, 5 were anaplastic large-cell lymphomas, 1 Lennert lymphoma, and 8 T-cell lymphomas (other). CD37 was not detected in 58 of 58 Hodgkin lymphoma samples. Flow cytometry was used to assess expression of CD37 in leukemia samples. Figure 2B (left) shows that 58 of 58 human CLL samples had an MFIR for CD37 expression of >2 and a mean MFIR of 83. The expression was heterogeneous. This observation was in line with previously reported data in B-cell malignancies (1, 6, 18). During a bioinformatic search of the Broad-Novartis Cancer Cell Line Encyclopedia (19) for novel targets in AML, we discovered that some AML cell lines appeared to exhibit RNA expression of CD37. Because we did not expect this lymphoid marker to be expressed in myeloid cells, we sought to determine whether primary AML samples expressed CD37 at the protein level. Figure 2B (right) shows flow cytometry results for the expression of CD37 in 26 of 26 AML samples. Because AML is organized as a hierarchy sustained by LSCs that are typically found in the $CD34^+$ $CD38^-$ fraction, we analyzed the expression of CD37 in the myeloid blasts ($CD33^+$) and $CD34^+CD38^-$ LSCs from each sample, the mean MFIR values were 85 and 126 respectively. Interestingly, the expression of CD37 in $CD34^+$/$CD38^-$ stem cells of 15 additional AML samples versus 10 normal bone marrow samples

not only appeared to be differential ($P = 0.013$) but suggested that normal stem cells exhibit minimal to no CD37 expression (Fig. 2C).

Mechanism of action of AGS67E

AGS67E (Fig. 3A) is a fully human anti-CD37 monoclonal IgG2 antibody conjugated to the potent microtubule-disrupting agent MMAE via reduced cysteines and the protease-cleavable linker maleimidocaproyl-valine-citrulline-p-aminobenzy-loxycarbonyl. The affinity (EC_{50}) and cytotoxicity (IC_{50}) of AGS67E to human B cells was 0.16 nmol/L and 17 nmol/L, respectively (Supplementary Fig. S1), and we have shown that, upon binding to CD37, this ADC internalizes within 100 minutes, as confirmed using flow cytometry (Supplementary Fig. S2). We have also determined that the unconjugated antibody of AGS67E (AGS67C) did not exhibit antitumor efficacy (Supplementary Fig. S3) nor did it induce ADCC *in vitro* (Supplementary Fig. S4). Methods used for Supplementary Figs. S1–S4 can be found in the supplementary data.

In an effort to better characterize the *in vitro* mechanism of action of AGS67E, its ability to alter cell viability/proliferation, cell-cycle progression, and apoptosis was assessed. Table 1 summarizes the *in vitro* cytotoxicity of AGS67E in cell lines representing NHL, CLL, and AML. With the exception of Rec-1, all NHL cell lines were responsive to AGS67E activity that ranged in IC50 from ∼0.04 to 20 nmol/L. For CLL, JVM-3 cells were tested with a mean IC50 of 0.50 nmol/L. A mean IC50 of ∼0.1 to 5.7 nmol/L was observed for 7 different AML cell lines. AGS67E was also not cytotoxic in an additional 9 AML cells lines. CD37 was expressed by all cell lines tested, with the exception of MOLT-4 (ALL) cells that were used as a CD37-negative cell line control. Figure 3B shows examples of the survival curves for a subset of cell lines shown in Table 1.

In comparison with an isotype ADC control, AGS67E consistently altered cell-cycle progression in CD37-positive cell lines representing NHL, CLL, and AML, while showing no appreciable change in the cell cycle of Hel92.1.7 AML cells (Fig. 3 and Table 2) that had been shown not to be responsive to AGS67E cytotoxicity *in vitro* (Fig. 3B and Table 1). In each cell line (Mino, MV4–11, or JVM-3), AGS67E treatment resulted in a substantial increase in cells in the G_2–M phase of the cell cycle, while in turn leading to significant decreases in cells that resided in the G_0–G_1 or S phases prior to AGS67E treatment. Overall, the relative impact of AGS67E treatment on cell-cycle progression appeared greater in the leukemia lines than in the Mino lymphoma cells. Further, the effect of AGS67E on the MV4–11 AML cell line was greater than that on the JVM-3 CLL cell line. These observations did not correlate with relative doubling times of the cell lines. For reference, free MMAE payload, DMSO, and no treatment groups were included in the analysis.

As was seen with the ability of AGS67E to induce cytotoxicity, the ability of AGS67E to induce apoptosis was also consistent across the Mino, MV4–11, and JVM-3 cell lines (Table 3). In comparison with the control ADC, AGS67E demonstrated greater relative Annexin V staining in the MV4–11 AML cell line (9.9-fold increase) versus JVM-3 and Mino, which exhibited a ∼3-fold increase in Annexin V positivity. These observations also did not correlate with relative doubling times of the cell lines.

Efficacy of AGS67E in NHL and CLL cell line xenografts

Because *in vitro* drug-response assays do not always reflect the *in vivo* setting, we turned to xenografting. Table 4 summarizes the efficacy of AGS67E in a variety of NHL, CLL, and AML cell line xenografts. Although different dosing and schedules were used, efficacy was observed with every lymphoma xenograft; AGS67E appeared to show a greater absolute effect in the leukemic xenografts with 3 of 6 showing tumor stasis or complete regression and tumor-free animals. However, 2 of 6 of the AML xenografts also showed tumor growth inhibition that was <50%, and Hel.92.1.7 showed no antitumor activity following AGS67E treatment. As with *in vitro* activity of AGS67E, the levels of CD37 did not show a correlation with *in vivo* activity. Figure 4A shows the antitumor efficacy of AGS67E in a Rituxan-resistant Burkitt lymphoma line, Ramos-RR-Xcl. A correlation between efficacy and dose was observed with 3 mg/kg, QW×2 showing tumor regressions. With respect to leukemias, Fig. 4B shows potent antitumor efficacy with 1.5 and 3 mg/kg, QW×3 showing tumor regressions in CLL JVM-3 xenografts. The most potent *in vivo* activity with AGS67E occurred with the MV4–11 AML xenografts (Fig. 4C) dosed with 0.75, 1.5, and 3 mg/kg, QW× 4 with tumor regressions observed in 26 of 27 xenografts and tumor eradication in 20 of 27 mice. AGS67E did not lead to lethality or body-weight loss during any of the *in vivo* studies conducted.

Efficacy of AGS67E in patient-derived orthotopic AML xenografts

To determine whether AGS67E could inhibit orthotopic AML xenografts, we turned to patient-derived samples. Figure 5A shows the experimental design to evaluate the ability of AGS67E to inhibit established and disseminated growth of patient-derived orthotopic AML xenografts. Briefly, we injected AML patient-derived peripheral blood into the right femur and allowed establishment and outgrowth, as well as dissemination following measurement of engraftment into the left femur and two tibias (aka bone marrow). Figure 5B summarizes the effect of AGS67E to inhibit established growth of 4 patient-derived AML samples in the RF versus the disseminated bone marrow. The 4 AML samples used (patient samples 1–4) were newly diagnosed, and their FAB subtypes were M1, M5b, M5a, and M5a respectively. In every sample, the engraftment and outgrowth of patient-derived AML occurred in the presence of the control ADC with a range of 22% to 100% in the right femur and a range of 3% to 52% in the disseminated bone marrow. For AGS67E-treated mice, engraftment and outgrowth in the right femur and disseminated bone marrow was significantly lower and ranged from 0% to 38% and 0% to 18%, respectively. Moreover, in 3 of 4 of these samples, AML cells were undetectable after AGS67E treatment in right femur or disseminated bone marrow. The MFIR of CD37 expression is also shown for the $CD33^+$ blasts and $CD34^+/CD38^-$ LSC. A correlation between AGS67E activity and CD37 levels was not observed.

Discussion

Within the context of antibody-based therapeutics, hematologic malignancies are frequently targeted. While Rituxan and CD20 targeting have paved the way for treating B-cell malignancies (7, 8), resistance to Rituxan has led to the evaluation of other cell surface targets and a variety of non–antibody- and antibody-based therapeutics (20–22), one such target is CD37. Currently, three publically disclosed antibody therapeutics that target CD37

are in clinical development (11–13). These include naked antibodies as well as a recently reported ADC (13). Interestingly, all of these antibodies are human IgG1 isotypes with enhanced ADCC activity that has been reported, in addition to apoptosis induction, as integral to their mechanism of action.

Here, we introduce AGS67E, the first fully human anti-CD37 monoclonal IgG2k antibody conjugated to the potent microtubule-disrupting agent MMAE, via reduced cysteines and the protease-cleavable linker maleimidocaproyl-valine-citrulline-p-aminobenzyloxycarbonyl. We have shown that this ADC has high affinity for and rapidly internalizes CD37, and that it is cytotoxic, apoptotic, and alters the cell cycle of cell lines representing NHL and CLL *in vitro*. We also showed that AGS67E inhibits growth of several xenografts representing NHL and CLL.

In contrast with the other reported anti-CD37 therapeutics, the unconjugated antibody component (AGS67C) of our ADC has not exhibited antitumor activity, nor has it demonstrated appreciable apoptotic or cytotoxic activity. AGS67C was selected for its ability to optimally and potently deliver the MMAE payload of AGS67E. Because AGS67C is a fully human IgG2, we observed very low ADCC activity *in vitro* using PBMCs, but demonstrated increased ADCC activity when the isotype of this antibody was switched to human IgG1. Because the preclinical potency of our agent is similar or superior to the reported preclinical efficacy of other CD37 antibodies in similar models of B-cell malignancies (11–13), we postulated that adding ADCC and apoptosis-inducing capability to the unconjugated antibody component of our ADC was unnecessary, and further that it could prove to be a liability from a toxicology or pharmacokinetic perspective when the drug is eventually tested in humans.

Using the unconjugated antibody that makes up AGS67E as well as another anti-CD37 antibody, 9a73.1, we have also confirmed previously reported expression of CD37 in malignant B cells, normal B cells, and in various PBMCs and in certain normal tissues where lymphocytes reside (1, 6). For the first time, we report that CD37 is also expressed in T-cell lymphomas, AML, and in AML $CD34^{+}CD38^{-}$ stem cells, while having minimal to no expression in normal $CD34^{+}CD38^{-}$ stem cells. Moreover, we report that AGS67E potently inhibits AML cell line and patient-derived samples *in vitro* and *in vivo* using subcutaneous and orthotopic/disseminated models. These data support a potential new therapeutic avenue for AGS67E and possibly for existing and new CD37 targeted therapeutics.

Interestingly, during these studies, we found some intriguing differences upon AGS67E targeting of NHL, CLL, and AML cell lines versus patient-derived samples. First, while the absolute *in vitro* sensitivity of NHL, CLL, and AML cell lines to AGS67E generally correlated with *in vivo* efficacy, there was not a direct rank-order correlation between *in vitro* and *in vivo* efficacy, nor was there a tight correlation with CD37 levels. Despite expressing significant CD37 levels, AGS67E was less efficacious in some cell lines and, although not fully understood, may be attributable to inabilities of ADC internalization and/or processing as well as resistance. Second, the *in vitro* potency of AGS67E in AML cell lines was approximately an order of magnitude less than in NHL cell lines. Initially, we speculated that this was due to CD37 levels being approximately an order of magnitude

lower in AML versus NHL cell lines and xenografts, but the *in vivo* potency in AML xenografts appeared greater than that of NHL xenografts, with tumor regressions and a higher incidence of tumor-free mice observed. Third, in contrast with NHL and CLL cell lines, where nearly all were sensitive to AGS67E *in vitro* and *in vivo*, the sensitivity of AML cell lines to AGS67E *in vitro* (7 of 16) and *in vivo* (3 of 5) was found to be more heterogeneous and is likely due to the genetic complexity and heterogeneity of AML as well as increased susceptibility of individual cell lines and xenografts to AGS67E and its microtubule disrupting payload. This possibility is also extended to the NHL and CLL cell lines in which CD37 was expressed but where efficacy was not observed. Interestingly, when we tested AGS67E in patient-derived AML samples *in vivo*, 4 of 4 samples were potently inhibited by AGS67E, thus indicating that there may be differences in the susceptibility of extensively passaged AML cell lines versus fresh patient-derived AML samples to the effects of AGS67E. In any case, further investigation will be needed to predict response and extent of response to AGS67E in AML as well as in NHL and CLL.

Taken together, the potent activity exhibited by AGS67E highlights its therapeutic potential in B/T-cell malignancies and AML and supports its current clinical development. To our knowledge, this body of work is also the first demonstration that CD37 is well expressed in T-cell lymphomas and AML and that CD37 is a potential drug target in these diseases.

Supplementary Material

Refer to Web version on PubMed Central for supplementary material.

Acknowledgments

The authors thank the hardworking and thoughtful members of the Agensys research departments that did not appear on this paper, but that significantly contributed to historical data and prior conference presentations that ultimately led to this final article. The authors are also grateful to have utilized the ADC technology licensed from Seattle Genetics Inc.

Grant Support

J.E. Dick and T.J. Kipps received funding from Agensys Inc. through a material transfer agreement.

References

1. Link MP, Bindl J, Meeker TC, Carswell C, Doss CA, Warnke RA, et al. A unique antigen on mature B-cells defined by a monoclonal antibody. J Immunol. 1986; 137:3013–3018. [PubMed: 3489782]
2. Schwartz-Albiez R, Dorken B, Hofmann W, Moldenhauer G. The B cell-associated CD37 antigen (gp40–52). Structure and subcellular expression of an extensively glycosylated glycoprotein. J Immunol. 1988; 140:905–914. [PubMed: 3257508]
3. Lapalombella R, Yeh YY, Wang L, Ramanunni A, Rafiq S, Jha S, et al. Tetraspanin CD37 directly mediates transduction of survival and apoptotic signals. Cancer Cell. 2012; 21:694–708. [PubMed: 22624718]
4. van Spriel AB, Puls KL, Sofi M, Pouniotis D, Hochrein H, Orinska Z, et al. A regulatory role for CD37 in T cell proliferation. J Immunol. 2004; 172:2953–2961. [PubMed: 14978098]
5. Knobeloch KP, Wright MD, Ochsenbein AF, Liesenfeld O, Löhler J, Zinkernagel RM, et al. Targeted inactivation of the tetraspanin CD37 impairs T-cell-dependent B-cell response under suboptimal costimulatory conditions. Mol Cell Biol. 2000; 20:5363–5369. [PubMed: 10891477]

6. Moore K, Cooper SA, Jones DB. Use of the monoclonal antibody WR17, identifying the CD37 gp40–45 Kd antigen complex, in the diagnosis of B-lymphoid malignancy. J Pathol. 1987; 152:13–21. [PubMed: 3305845]
7. Maloney DG. Anti-CD20 antibody therapy for B-cell lymphomas. N Engl J Med. 2012; 366:2008–2016. [PubMed: 22621628]
8. Owen CJ, Stewart DA. Obinutuzumab for B-cell malignancies. Expert Opin Biol Ther. 2014; 14:1197–1205. [PubMed: 24856933]
9. Press OW, Eary JF, Badger CC, Martin PJ, Appelbaum FR, Levy R, et al. Treatment of refractory non-Hodgkin's lymphoma with radiolabeled MB-1 (anti-CD37) antibody. J Clin Oncol. 1989; 7:1027–1038. [PubMed: 2666588]
10. Kaminski MS, Fig LM, Zasadny KR, Koral KF, DelRosario RB, Francis IR, et al. Imaging, dosimetry, and radioimmunotherapy with iodine 131-labeled anti-CD37 antibody in B-cell lymphoma. J Clin Oncol. 1992; 10:1696–1711. [PubMed: 1403053]
11. Zhao X, Lapalombella R, Joshi T, Cheney C, Gowda A, Hayden-Ledbetter MS, et al. Targeting CD37-positive lymphoid malignancies with a novel engineered small modular immunopharmaceutical. Blood. 2007; 110:2569–2577. [PubMed: 17440052]
12. Heider KH, Kiefer K, Zenz T, Stilgenbauer S, Ostermann E, Baum A, et al. A novel Fc-engineered monoclonal antibody to CD37 with enhanced ADCC and high proapoptotic activity for treatment of B-cell malignancies. Blood. 2011; 118:4159–4168. [PubMed: 21795744]
13. Deckert J, Park PU, Chicklas S, Yi Y, Li M, Lai KC, et al. A novel anti-CD37 antibody-drug conjugate with multiple anti-tumor mechanisms for the treatment of B-cell malignancies. Blood. 2013; 122:3500–3510. [PubMed: 24002446]
14. Senter PD, Sievers EL. The discovery and development of brentuximab vedotin for use in relapsed Hodgkin lymphoma and systemic anaplastic large cell lymphoma. Nat Biotechnol. 2012; 30:631–637. [PubMed: 22781692]
15. Verma S, Miles D, Gianni L, Krop IE, Welslau M, Baselga J, et al. Trastuzumab emtansine for HER2-positive advanced breast cancer. N Engl J Med. 2012; 367:1783–1791. [PubMed: 23020162]
16. Murphy AJ, Macdonald LE, Stevens S, Karow M, Dore AT, Pobursky K, et al. Mice with megabase humanization of their immunoglobulin genes generate antibodies as efficiently as normal mice. PNAS. 2014; 111:5153–5158. [PubMed: 24706856]
17. Doronina SO, Toki BE, Torgov MY, Mendelsohn BA, Cerveny CG, Chace DF, et al. Development of potent monoclonal antibody auristatin conjugates for cancer therapy. Nat Biotechnol. 2003; 21:778–784. [PubMed: 12778055]
18. Barrena S, Almeida J, Yunta M, Lopez A, Fernandez-Mosteirin N, Giralt M, et al. Aberrant expression of tetraspanin molecules in B-cell chronic lymphoproliferative disorders and its correlation with normal B-cell maturation. Leukemia. 2005; 19:1376–1383. [PubMed: 15931266]
19. Barretina J, Caponigro G, Stransky N, Venkatesan K, Margolin AA, Kim S, et al. The cancer cell line encyclopedia enables predictive modelling of anticancer drug sensitivity. Nature. 2012; 483:603–607. [PubMed: 22460905]
20. Danilov AV. Targeted therapy in chronic lymphocytic leukemia: past, present and future. Clin Ther. 2013; 35:1258–1270. [PubMed: 24054703]
21. Scott AM, Wolchok JD, Old LJ. Antibody therapy of cancer. Nat Rev Cancer. 2012; 12:278–287. [PubMed: 22437872]
22. Palanca-Wessels MC, Press OW. Advances in the treatment of hematologic malignancies using immunoconjugates. Blood. 2014; 123:2293–2301. [PubMed: 24578502]

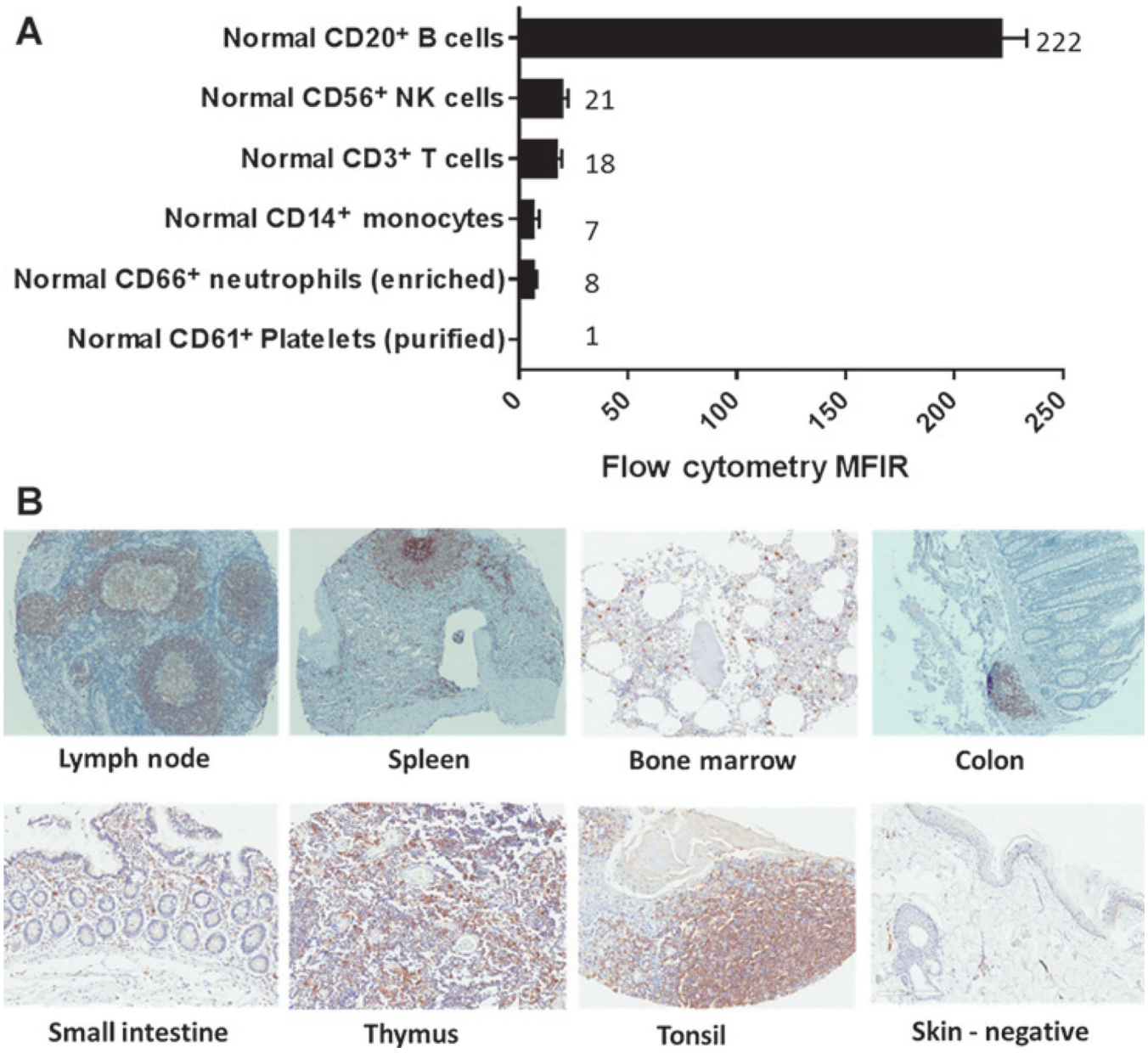

Figure 1.

Expression of CD37 in PBMCs and normal tissue. A, flow-cytometric analysis was performed to assess the ability of AGS67C to bind to assorted PBMCs and to quantitate the level of CD37 expressed and represented as an MFIR. B, 9a73.1, an anti-CD37 antibody capable of detecting CD37 in FFPE tissue, was utilized to reveal its expression in the normal tissues shown. Normal skin was used as a negative control for CD37 expression.

A

Cancer	Numbers of cases in each final score category				Overall positive ratio	Total cases
	Strong	Moderate	Low	Negative		
B-cell NHL	113	48	10	30	85%	201
T-cell lymphoma	7	3	4	3	82%	17
Hodgkin lymphoma	0	0	0	58	0%	58
Total	120	51	14	91	67%	276

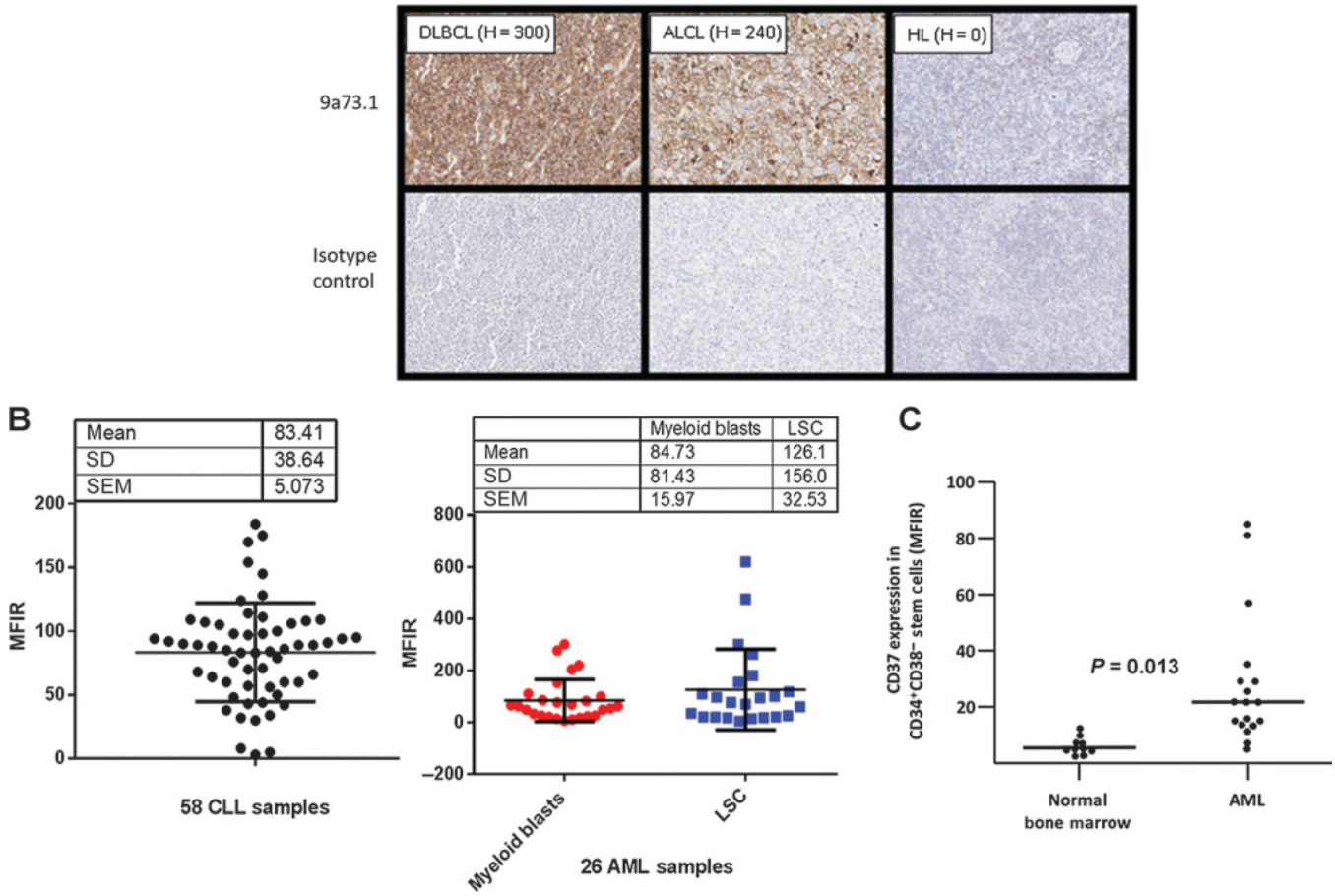

Figure 2.

Expression of CD37 in B/T-cell lymphomas, Hodgkin lymphoma, CLL, and AML. A, IHC of patient-derived B/T-cell lymphomas as well as Hodgkin lymphoma. 9a73.1 antibody was used to assess CD37 expression in FFPE patient-derived tumor samples. H-score was employed to calculate positivity by summing the percentage of tumor cells stained at a given staining intensity (0, negative; 1, weak; 2, moderate; 3, strong) multiplied by the weighted intensity. The results shown in the table are assigned into one of four groups according to their H-score as follows: high, 201–300; moderate, 101–200; low: 1–100; and negative, 0. The collage shows examples of CD37 staining in B- and T-cell lymphoma samples as well as negative staining in a Hodgkin lymphoma sample. B, flow cytometric analysis was performed to assess the ability of AGS67C to bind to 58 patient-derived CLL samples (left) and 26 AML samples (right). For the AML samples, CD37 expression is shown in $CD33^{+}$ myeloid blasts as well as $CD34^{+}CD38^{-}$ LSCs. C, a comparison of CD37 expression was also performed in $CD34^{+}CD38^{-}$ leukemic and normal stems cells from 15 and 10 patients,

respectively. MFIRs are reported. The difference observed between the mean expression of CD37 in $CD34^+/CD38^-$ LSCs versus normal stem cells was statistically significant (P = 0.013; independent two-sample Student t test).

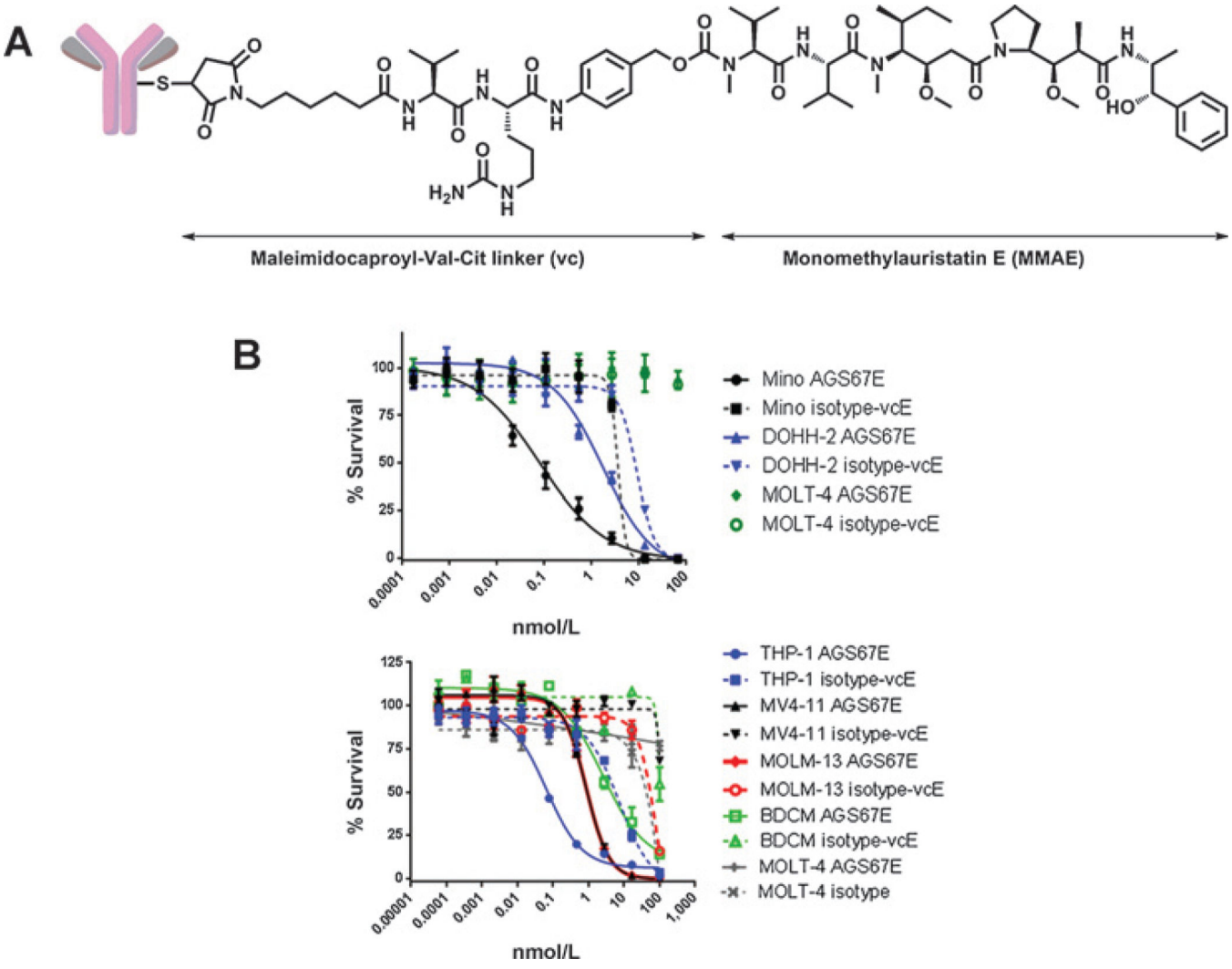

Figure 3.

Structure and *in vitro* characterization of AGS67E, an anti-CD37 ADC. A, structure of AGS67E (17). AGS67E induces cytotoxicity (B; Table 1), cell-cycle alterations (Table 2), and apoptosis (Table 3) in NHL, CLL, and AML cell lines. Assays were performed in the presence of AGS67E or control ADC, and Presto Blue Reagent was used to measure cell viability after 5 days, Hoechst 33342 was used to measure cell-cycle progression after 1 day, and Annexin V/7-AAD was used to measure apoptosis and necrosis after 1 day.

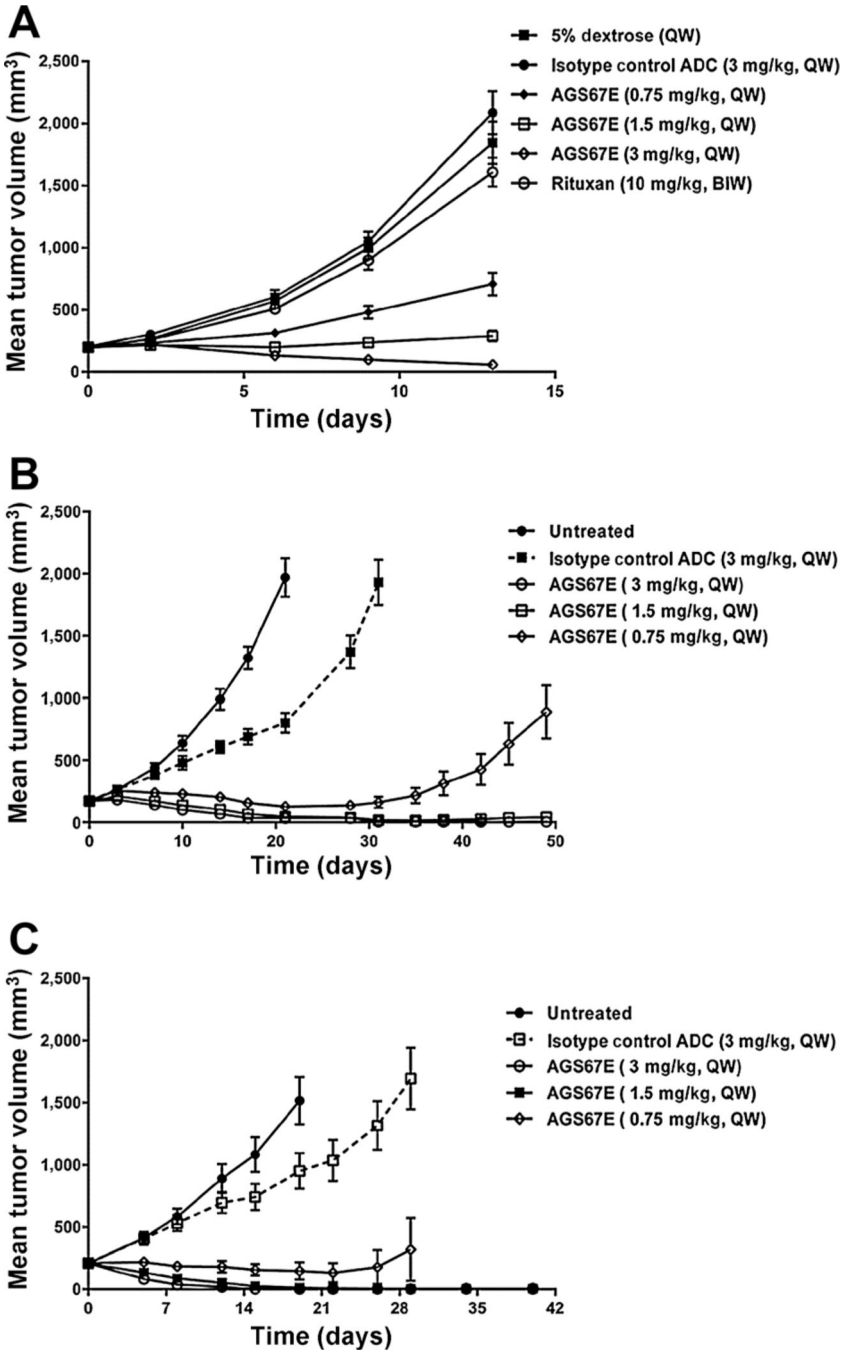

Figure 4.

Antitumor efficacy of AGS67E in established subcutaneous NHL, CLL, and AML cell line xenografts. A tabular summary of the *in vivo* efficacy of AGS67E in 10 cell line xenograft models is shown in Table 4, where the acronyms MFIR and TGI (tumor growth inhibition) were used to describe CD37 expression and the antitumor activity of AGS67E versus controls. Examples of the tumor growth curves and antitumor efficacy of AGS67E are shown for the following xenografts: Ramos-RR-XcL, a Rituxan-resistant lymphoma

xenograft; Ramos-RR-XcL (A); JVM-3, a CLL xenograft (B); and MV4–11, an AML xenograft (C).

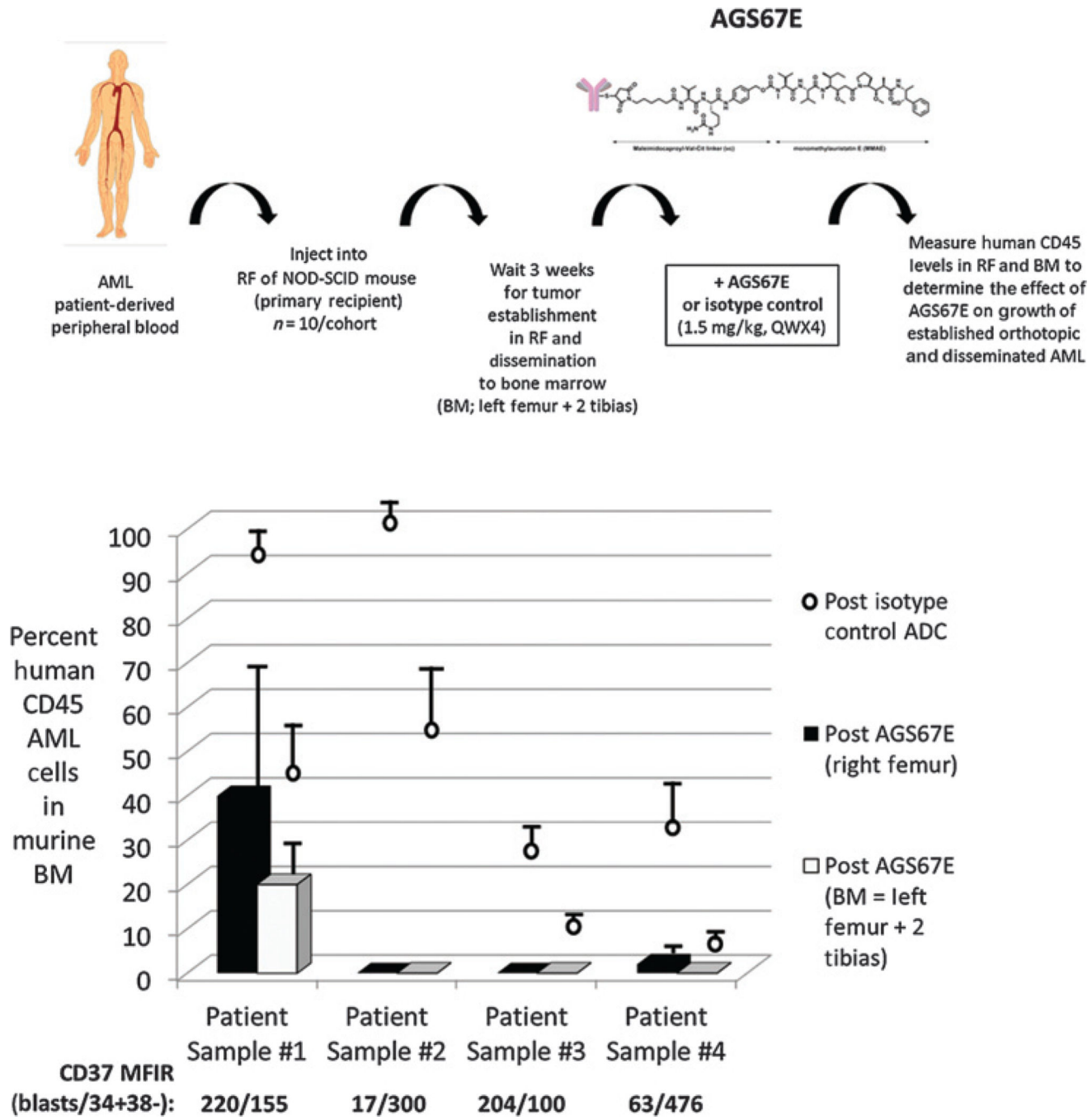

Figure 5.

Antitumor efficacy of AGS67E in established orthotopic patient-derived AML xenografts. A, experimental design used to evaluate the ability of AGS67E to inhibit established and disseminated growth of patient-derived orthotopic AML xenografts. Patient-derived AML peripheral blood was injected into the right femur (RF) of NOD/SCID mice and allowed to establish and disseminate into the left femur and 2 tibias (aka bone marrow, BM). Human CD45 levels were used to monitor the extent of AML engraftment and outgrowth. B, antitumor efficacy of AGS67E in 4 established and disseminated orthotopic patient-derived

AML xenografts. All AGS67E versus control ADC comparisons were statistically significant ($P < 0.0001$; independent two-sample Student *t* test).

Table 1

AGS67E is cytotoxic to NHL, CLL, and AML cells *in vitro*

Cell line	Classification	IC_{50} (nmol/L)	CD37 MFIR
NHL			
Daudi	Burkitt lymphoma	0.078 ± 0.02	39
Ramos	Burkitt lymphoma	0.047 ± 0.03	534
Mino	Mantle cell lymphoma	0.07 ± 0.49	301
Granta-519	Mantle cell lymphoma	0.79 ± 0.61	372
REC-1	Mantle cell lymphoma	No cytotoxicity	341
DOHH-2	Follicular cell lymphoma	0.98 ± 1.1	581
SU-DHL-4	Diffuse large B-cell lymphoma	0.23 ± 0.30	662
WSU-DLCL2	Diffuse large B-cell lymphoma	19.7 ± 3.0	554
CLL			
JVM-3	Chronic lymphocytic leukemia	0.50 ± 0.72	129
AML			
THP-1	FAB M5	0.13 ± 0.08	23
SKM-1	FAB M5	0.71 ± 0.20	30
MV4–11	FAB M5	1.2 ± 0.9	22
MOLM-13	FAB M5a	1.3 ± 0.5	25
OCI-AML2	FAB M4	1.1 ± 0.6	18
Kasumi-1	FAB M2	3.5 ± 0.7	9
BDCM	FAB M5a	5.7 ± 1.6	64
PL-21	FAB M3	No cytotoxicity	4
EoL-1	Eosinophilic	No cytotoxicity	3
HL-60	FAB M2	No cytotoxicity	5
UT-7	FAB M7	No cytotoxicity	10
KG-1	Erythroleukemia macrophage	No cytotoxicity	20
CMK	FAB M7 (megakaryocytic)	No cytotoxicity	11
Tf-1a	Erythroleukemia FAB M6	No cytotoxicity	26
Hel 92.1	Erythroleukemia	No cytotoxicity	82
ALL			
MOLT-4	T-cell leukemia	No cytotoxicity	1

Table 2

AGS67E induces cell-cycle alterations in NHL, CLL, and AML cell lines *in vitro*

			40 nmol/L (24 h)		
Total population, %	**No treatment**	**DMSO**	**AGS67E**	**Isotype ADC**	**MMAE**
Mino (NHL)					
Sub-G_1	1.51	1.61	4.05	2.08	2.77
G_0–G_1	59.5	57.6	46.8	55.6	47.2
S	22.8	23.5	16.7	22	15.1
G_2–M	15.7	16.9	32.2	19.9	34.5
MV4–11 (AML)					
Sub-G_1	0.28	0.22	0.80	0.30	0.59
G_0–G_1	66.4	70.2	41.8	66.5	26.6
S	14.1	11.9	8.32	11.8	14.9
G_2–M	19.3	17.9	49.1	21.7	57.1
JVM-3 (CLL)					
Sub-G_1	4.24	2.69	5.19	1.36	8.96
G_0–G_1	67.1	67.4	56.7	68.7	36.7
S	12.5	13.6	9.88	14	10.8
G_2–M	14.7	14.9	25.3	14.7	38.5
Hel92.1.7 (AML)					
Sub-G_1	12.3	8.66	2.46	2.53	1.95
G_0–G_1	48.5	51	51	48.8	26.9
S	18.8	19.2	19.8	19.8	14.5
G_2–M	20.1	20.8	26.2	28.4	54.3

Table 3

AGS67E induces apoptosis in NHL, CLL, and AML cell lines *in vitro*

			40 nm (24 h)		
Total population, %	**No treatment**	**DMSO**	**AGS67E**	**Isotype ADC**	**MMAE**
Mino (NHL)					
Annexin V	24.6	24.2	85.4	29.1	94.6
Sytox AADvanced	15.8	14.9	32.7	15.9	59.5
Annexin V/Sytox AAD	15.6	14.8	31.4	15.7	57.2
Unstained (live)	75.3	75.6	13.3	70.7	3.1
MV4–11 (AML)					
Annexin V	4.4	4.7	39.6	4.0	78.1
Sytox AADvanced	2.6	3.1	6.6	2.4	28.6
Annexin V/Sytox AAD	2.3	2.4	6.4	2.2	27.2
Unstained (live)	95.6	94.7	60.2	95.8	20.4
JVM-3 (CLL)					
Annexin V	18.0	18.0	49.7	16.8	58.2
Sytox AADvanced	13.7	12.9	38.1	12.6	40.3
Annexin V/Sytox AAD	12.9	12.1	34.5	11.8	37.0
Unstained (live)	81.2	81.2	46.7	82.4	38.6
Hel92.1.7 (AML)					
Annexin V	17.5	17.8	18.4	18.1	37.3
Sytox AADvanced	14.8	14.8	15.2	15.4	18.9
Annexin V/Sytox AAD	13.3	13.5	13.8	13.9	17.2
Unstained (live)	81.1	81.0	80.2	80.4	61.0

Table 4

Summary of antitumor activity of AGS67E in NHL, CLL, and AML cell line xenografts

Xenograft cell line	Cancer type	CD37 (MFIR)	*In vitro* cytotox (IC_{50}, nmol/L)	Dose/schedule	TGI (%)
Mino	MCL	300	0.07	0.5 mg/kg, BIWx4	92
				0.25 mg/kg, BIWx4	51
DOHH2	FL	580	0.98	3.0 mg/kg, Q1Wx2	95
				1.5 mg/kg, Q1Wx2	66
				0.75 mg/kg, Q1Wx2	27
WSU-DLCL2	DBCL	554	19.7	1.5 mg/kg, BIWx4	96
				0.75 mg/kg, BIWx4	31
Ramos-RR-XcL	Burkitt lymphoma	140	0.01	3.0 mg/kg, Q1Wx2	97
				1.5 mg/kg, Q1Wx2	86
				0.75 mg/kg, Q1Wx2	63
JVM3	CLL	129	0.50	3.0 mg/kg, Q1Wx3	123
				1.5 mg/kg, Q1Wx3	120
				0.75 mg/kg, Q1Wx3	108
MV-4–11	AML	22	1.2	3.0 mg/kg, Q1Wx4	116
				1.5 mg/kg, Q1Wx4	115
				0.75 mg/kg, Q1Wx4	108
MOLM-13	AML	25	1.3	3.0 mg/kg, Q1Wx2	106
				1.5 mg/kg, Q1Wx2	103
				0.75 mg/kg, Q1Wx2	69
THP-1	AML	23	0.1	1.5 mg/kg, Q1Wx3	95
KG-1	AML	20	No cytotoxicity	3.0 mg/kg, Q1Wx3	41
Hel 92.1.7	AML	82	No cytotoxicity	3.0 mg/kg, Q1Wx3	0